Supporting information

Silver(I)-Iodine Cluster with Efficient Thermally Activated Delayed Fluorescence and Suppressed Concentration Quenching

Xiao Li [a,b,d], Shan-Yue Wei [a,b,e], Dong-Hai Zhang [a,b], Jia-Xuan Hu [a,b], Chen-Lu Hou [a,b,d], Ting-Ting Lin [a,b], Xu-Lin Chen [a,b,c,d], Can-Zhong Lu [a,b,c,d]**

[a] State Key Laboratory of Structural Chemistry, Fujian Institute of Research on the Structure of Matter, Chinese Academy of Sciences, Fuzhou, Fujian 350002, China

[b] Xiamen Key Laboratory of Rare Earth Photoelectric Functional Materials, Xiamen Institute of Rare Earth Materials, Haixi Institutes, Chinese Academy of Sciences, Xiamen, Fujian 361021, China

[c] Fujian Science & Technology Innovation Laboratory for Optoelectronic Information of China, Fuzhou, Fujian 350108, China

[d] Fujian Normal University, Fuzhou City, Fujian Province 350007, China

[e] Engineering Research Center of Environment-Friendly Functional Materials, Ministry of Education, Institute of Materials Physical Chemistry, Huaqiao University, Xiamen 361021, PR China

*** Corresponding authors**

Xu-Lin Chen, E-mail: xlchem@fjirsm.ac.cn

Can-Zhong Lu, E-mail: czlu@fjirsm.ac.cn

1. General Information

All air and moisture sensitive reactions are carried out in an argon atmosphere. Unless otherwise specified, all starting materials used are commercially available and require no further purification. The reaction solvents used in the reaction are all commercial analytical pure reagents, and some of the reagents have been dried by molecular sieve (4 Å) before use. The prepared TADF material is twice dried and recrystallized before the device is manufactured. ^{1}H NMR, ^{31}P and ^{13}C NMR were obtained using a Bruker Avance III nuclear magnetic resonance spectrometer at a frequency of 500 Hz in deuterated chloroform ($CDCl_3$). Thermogravimetric analysis (TGA) was performed by TGA in a nitrogen atmosphere at a heating rate of 10 K/min. Single crystal X-ray diffraction data were collected on a Bruker-D8 VENTRUE diffractometer with an X-ray source of Mo kα. Cyclic voltammetry was performed with a scan rate of 50 mV/s at room temperature in anhydrous and argon-saturated dichloromethane solutions of 0.1 M tetrabutylammonium hexafluorophosphate and 1.0 mM investigated cluster with a CHI840D electrochemical analyzer. Glassy carbon, platinum wire and Ag/Ag^{+} (0.01 M of $AgNO_3$ in acetonitrile) were selected as the working electrode, auxiliary electrode and reference electrode, respectively. The ferrocenium/ferrocene couple was used as an internal standard. The UV-VIS absorption spectra were recorded by Agilent Cary 5000 UV-VIS spectrophotometer under ambient conditions. Fluorescence quantum yields were measured using FluoroMax-4 fluorescence spectrometers equipped with integrating spheres. Xenon lamp was used as a light source to record the steady-state PL spectra on Edinburgh FLS980. Using NT242-1K OPO laser as excitation source, the transient PL attenuation curves of samples were recorded in time-dependent single photon counting mode at Edinburgh FLS980.

2. Material Synthesis and Characterizatio

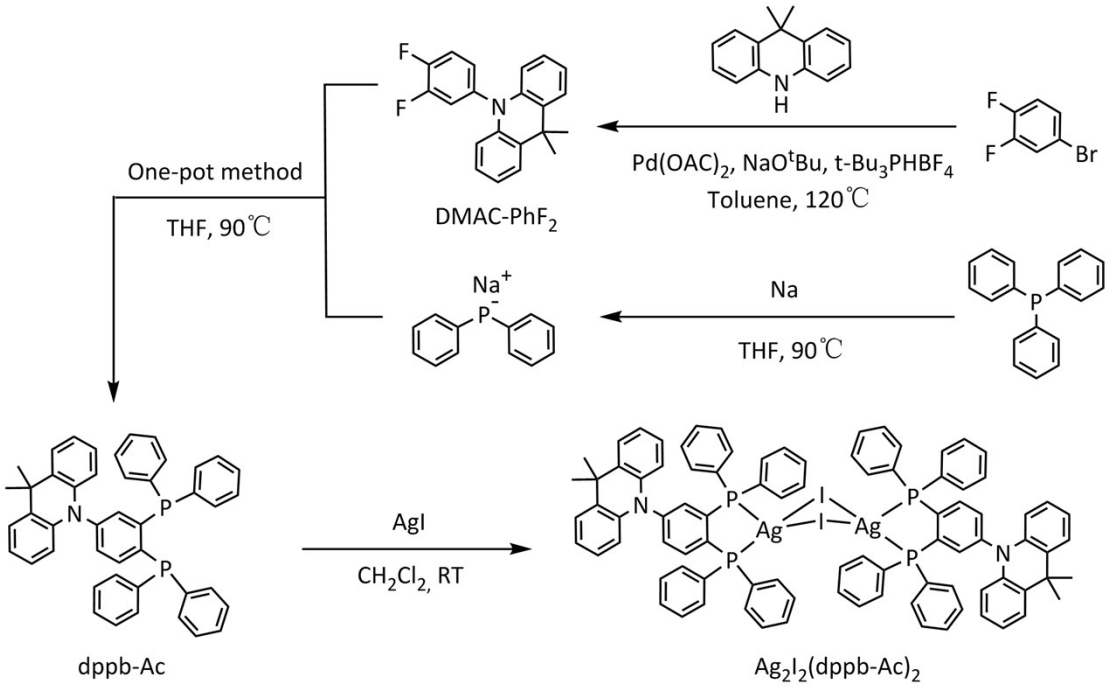

Scheme S1. Synthetic route of Ag_2I_2(dppb-Ac)$_2$

2.1 Synthesis of DMAC-PhF$_2$[1]

In a 500 ml three-neck flask, 3.86 g (20 nmol) of 4-bromo-1,2-difluorobenzene, 4.19 g (20 nmol) of 9,10-dihydro-9,9-dimethylacridine, 1.92 g (20 nmol) of sodium tert-butoxide, 0.29 g (1 nmol) of tri-tert-butylphosphonium tetrafluoroborate, 0.55 g (0.6 nmol) of tris(dibasic benzylacetone) dipalladium, with 100 ml of dry toluene as solvent, and stirred at reflux for 12 h at 120°C under argon atmosphere. The extracted organics were washed with ethyl acetate and saturated saline and dried by adding $MgSO_4$. The desiccant was removed by filtration and the solvent was removed under vacuum to give a gray-brown solid. The residue was purified by chromatography on silica gel (petroleum ether/dichloromethane, 5:1) to give 5.52 g (86%) of white solid. ^{1}H NMR (500 MHz, Chloroform-*d*) δ 7.53 (dd, *J* = 7.6, 1.7 Hz, 2H), 7.51 – 7.44 (m, 1H), 7.29 – 7.24 (m, 1H), 7.17 (ddt, *J* = 8.3, 3.9, 2.0 Hz, 1H), 7.07 (td, *J* = 7.7, 1.7 Hz, 2H), 7.02 (td, *J* = 7.4, 1.4 Hz, 2H), 6.33 (dd, *J* = 8.1, 1.4 Hz, 2H), 1.75 (s, 6H).

2.2 Synthesis of dppb-Ac[2]

In a 200 ml round bottom flask, 4.72 g (18 nmol) of triphenylphosphine, 1.86 g (81 nmol) of sodium, with 50 ml of anhydrous tetrahydrofuran as a solvent, were stirred under reflux under argon atmosphere for 12 h. The cooled crimson solution was transferred to another dry 200 ml round bottom flask containing 1.93 g (6 nmol) of DMAC- PhF_2 in a refluxed under argon atmosphere for three hours and then stirred at room temperature for three hours. After completion of the reaction, an appropriate amount of methanol was added to the solution. The extracted organics were washed with ethyl acetate and saturated saline and dried by adding $MgSO_4$. The desiccant was removed by filtration and the solvent was removed in vacuum to give a yellowish brown solid. The residue was purified by chromatography on silica gel (petroleum ether/dichloromethane, 4:1) to give 1.96 g (50%) of white solid. ^{1}H NMR (500 MHz, Chloroform-*d*) δ 7.45 (dd, *J* = 7.8, 1.6 Hz, 2H), 7.33 (q, *J* = 2.5 Hz, 10H), 7.30 – 7.18 (m, 14H), 7.03 (td, *J* = 7.7, 1.6 Hz, 2H), 6.96 (td, *J* = 7.4, 1.3 Hz, 2H), 6.30 (dd, *J* = 8.2, 1.2 Hz, 2H), 1.63 (s, 6H). ^{13}C NMR (126 MHz, Chloroform-*d*) δ 146.70, 146.61, 146.48, 146.39, 144.23, 144.16, 144.00, 143.94, 141.93, 140.78, 137.15, 137.11, 136.79, 136.75, 136.71, 136.67, 136.59, 136.55, 136.51, 136.47, 136.30, 136.24, 134.23, 134.21, 134.09, 134.07, 133.72, 133.71, 133.58, 133.56, 131.61, 130.50, 128.73, 128.54, 128.50, 128.43, 128.38, 126.31, 124.94, 120.84, 114.15, 36.00, 30.43.

2.3 Synthesis of Ag_2I_2(dppb-Ac)$_2$

(117 mg,0.50 mmol) of AgI was added to a solution of CH_2Cl_2 (5 ml) containing (0.33 g,0.50 mmol) of dppb-Ac. The mixture was stirred at room temperature for 3 h. The reaction mixture was filtered and the solvent was removed in vacuo to give a yellow powder. The residue was purified by recrystallization with CH_2Cl_2 /ether to give 296 mg of yellow crystals. 65% yield. ^{1}H NMR (500 MHz, Chloroform-d) δ 7.40 (dd, J = 13.7, 5.8 Hz, 6H), 7.37 – 7.32 (m, 8H), 7.32 – 7.26 (m, 12H), 7.20 (t, J = 7.2 Hz, 4H), 7.15 – 7.08 (m, 12H), 7.05 – 6.98 (m, 12H), 6.94 (t, J = 7.5 Hz, 4H), 6.21 (dd, J = 8.1, 1.2 Hz, 4H), 1.59 (s, 12H). ^{13}C NMR (126 MHz, CDCl3) δ 144.94, 144.79, 144.76, 144.60, 142.68, 142.66, 140.97, 140.80, 140.78, 140.57, 137.11, 137.07, 134.33, 134.29, 134.23, 134.19, 134.15, 134.11, 134.05, 134.00, 132.15, 132.08, 132.05, 131.98, 131.82, 131.74, 131.72, 131.64, 131.61, 131.60, 130.79, 129.53, 129.46, 128.48, 128.45, 128.42, 128.40, 128.38, 128.35, 128.32, 128.30, 126.45, 125.07, 121.15, 114.36, 77.37, 77.12, 76.86, 65.90, 36.04, 30.53, 15.34. ^{31}P NMR (202 MHz,

$CDCl_3$) δ -19.59, -20.76. Elemental Analysis. calcd for $C_{90}H_{74}Ag_2I_2N_2P_4$: C 60.83%, H 4.20%, N 1.58%. Found: C 60.81%, H 4.27%, N 1.60%.

3. X-ray structure determination

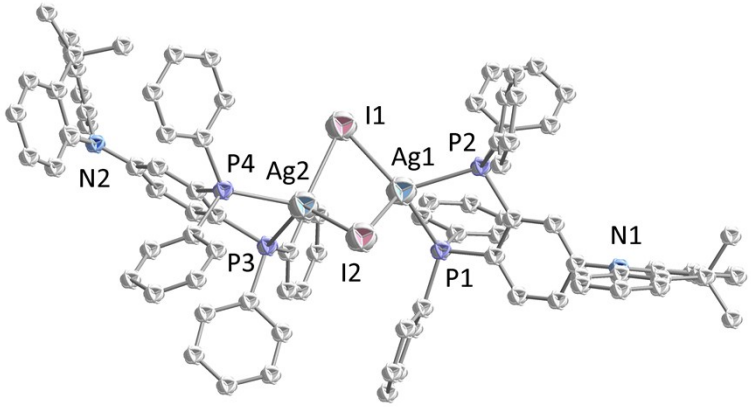

Figure S2. Crystal configuration of $Ag_2I_2(dppb\text{-}Ac)_2$

Table S1. Crystal parameters and refinement data of $Ag_2I_2(dppb\text{-}Ac)_2$

Compounds	$Ag_2I_2(dppb\text{-}Ac)_2$
Empirical formula	$C_{90}H_{74}Ag_2I_2N_2P_4$
Formula weight	1774.10
Temperature/K	200(2)
Crystal system	monoclinic
Space group	P21/c
a/Å	18.0702(5)
b/Å	13.9237(3)
c/Å	32.2579(8)
α/°	90
β/°	91.5860(10)
γ/°	90
Volume/Å3	8113.1(3)
Z	2
ρcalcg/cm3	1.559
μ/mm-1	1.469

F(000)	3804.0
Crystal size/mm3	0.14 × 0.13 × 0.11
Radiation	MoKα (λ = 0.71073)
2Θ range for data collection/°	3.884 to 55.894
Index ranges	-20 ≤ h ≤ 23, -18 ≤ k ≤ 18, -37 ≤ l ≤ 42
Reflections collected	58229
Independent reflections	19303 [Rint = 0.0497, Rsigma = 0.0545]
Data/restraints/parameters	19303/1335/1309
Goodness-of-fit on F2	1.038
Final R indexes [I>=2σ (I)]	R1 = 0.0430, wR2 = 0.0889
Final R indexes [all data]	R1 = 0.0811, wR2 = 0.1103
Largest diff. peak/hole / e Å-3	0.86/-0.81

Table S2. Selected bond length (Å) and bond angles (deg) of $Ag_2I_2(dppb\text{-}Ac)_2$

Ag1-I1	2.8012(5)
Ag1-I2	2.8723(5)
Ag1-P1	2.5253(12)
Ag1-P2	2.5271(11)
Ag2-I1	2.8825(4)
Ag2-I2	2.7756(4)
Ag2-P3	2.5161(11)
Ag2-P4	2.5113(11)
Ag1-Ag2	2.9981(5)
Ag1-I1	2.8012(5)
Ag1-I2	2.8723(5)
Ag1-P1	2.5253(12)
Ag1-P2	2.5271(11)
Ag2-I1	2.8825(4)
Ag2-I2	2.7756(4)

Ag2-P3	2.5161(11)
Ag2-P4	2.5113(11)
I1-Ag1-Ag2	59.493(11)
I1-Ag1-I2	107.585(14)
I2-Ag1-Ag2	56.384(11)
P1-Ag1-Ag2	114.15(3)
P1-Ag1-I1	129.64(3)
P1-Ag1-I2	105.02(3)
P1-Ag1-P2	80.36(4)
P2-Ag1-Ag2	164.12(3)
P2-Ag1-I1	117.06(3)
P2-Ag1-I2	115.30(3)
I1-Ag2-Ag1	56.853(11)
I2-Ag2-Ag1	59.518(11)
I2-Ag2-I1	108.004(14)
P3-Ag2-Ag1	115.19(3)
P3-Ag2-I1	105.96(3)
P3-Ag2-I2	129.36(3)
P4-Ag2-Ag1	159.77(3)
P4-Ag2-I1	107.95(3)
P4-Ag2-I2	121.66(3)
P4-Ag2-P3	80.42(4)
Ag1-I1-Ag2	63.654(11)
Ag2-I2-Ag1	64.098(11)

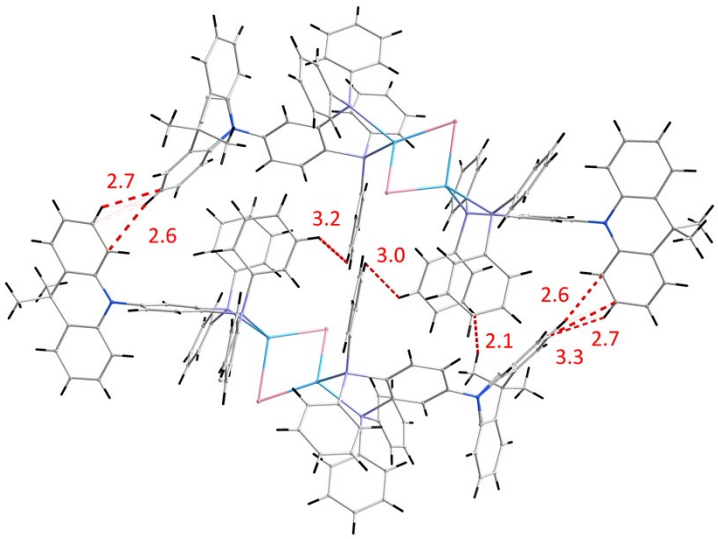

Figure S3. Single-crystal packing diagram of $Ag_2I_2(dppb\text{-}Ac)_2$.

4. Thermogravimetric Analysis (TGA)

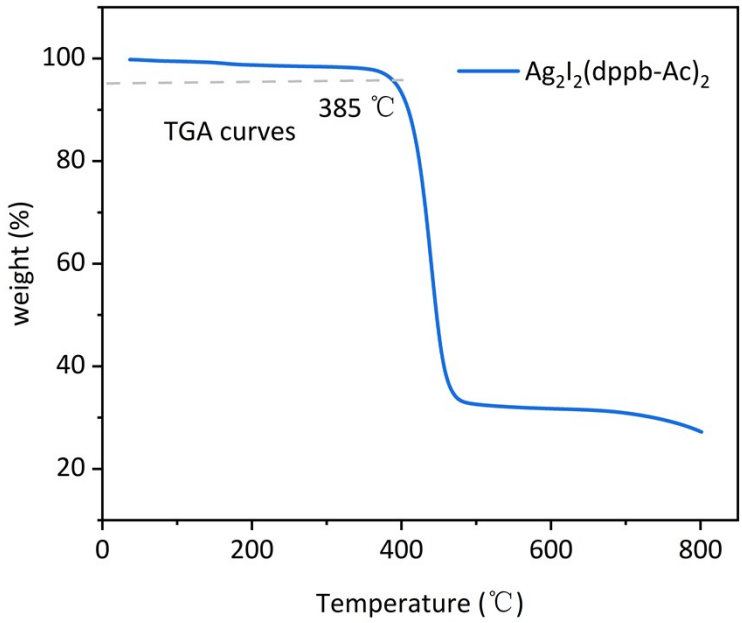

Figure S4. TGA curves of $Ag_2I_2(dppb\text{-}Ac)_2$. The Gray dashed line marks 95% of the original sample weight.

5. Cyclic Voltammetry

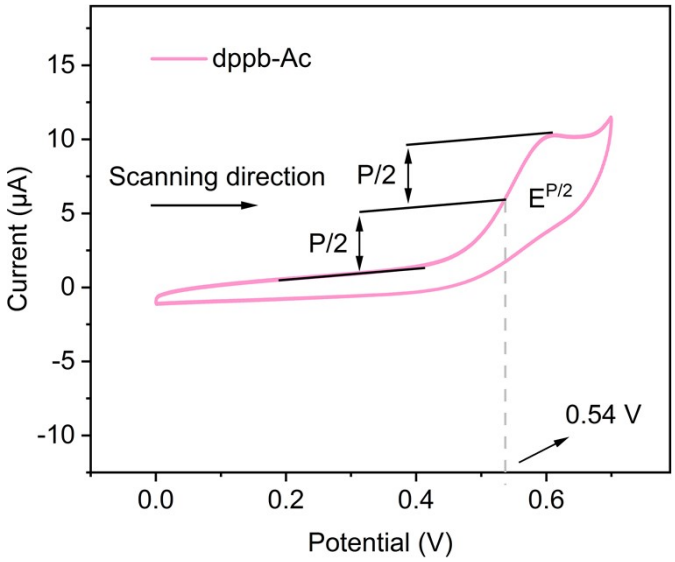

Figure S5. Cyclic voltammograms for the oxidation of dppb-Ac in dichloromethane at room temperature (scan range: 0—0.7 V, scan rate: 50 mV/s, concentration: 1 mM).

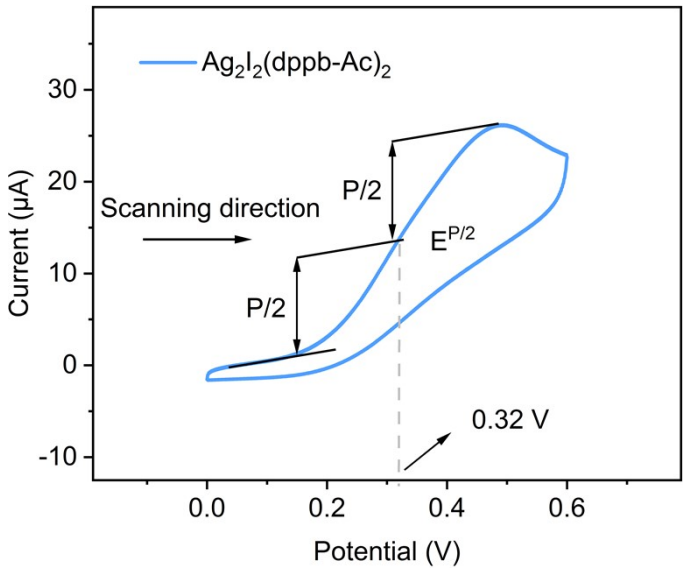

Figure S6. Cyclic voltammograms for the oxidation of $Ag_2I_2(dppb\text{-}Ac)_2$ in dichloromethane at room temperature (scan range: 0—0.6 V scan rate: 50 mV/s, concentration: 1 mM).

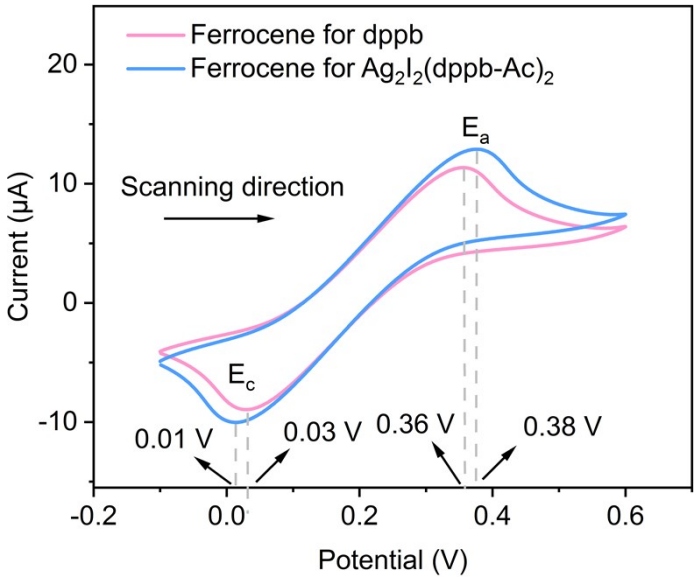

Figure S7. Cyclic voltammetry curves of ferrocene (internal standard).

Cyclic voltammetry was performed at room temperature in anhydrous and argon-saturated dichloromethane solutions of 0.1 M tetrabutylammonium hexafluorophosphate and 1.0 mM investigated compounds with a CHI840D electrochemical analyzer. Glassy carbon, platinum wire and Ag/Ag+(0.01 M of $AgNO_3$ in acetonitrile) were selected as the working electrode, auxiliary electrode and reference electrode, respectively. The ferrocenium/ferrocene couple was used as an internal standard. The HOMO and LUMO energy levels were estimated from the cyclic voltammetry and optical bandgaps (E_g) determined from the onset of the absorption band (λ_{onset}).

Table S3. Summary of CV data and energy levels.

Compound	E_{ox}[a] [ev]	$E_{FC/Fc+}$[b] [ev]	E_g[c] [ev]	E_{HOMO}[d] [ev]	E_{LUMO}[e] [ev]
dppb-Ac	0.54	0.20	3.10	-5.14	-2.04
Ag_2I_2(dppb-Ac)$_{2.}$	0.32	0.20	2.77	-4.92	-2.15

[a] The oxidation potentials (E_{OX}) were acquired by using the half-peak potentials determined as described in the literature[3] (Figure S5 and S6); [b] ferrocenium/ferrocene couple was used as an internal standard; [c] calculated from the absorption edge λonset using equation: $1241/\lambda_{onset}$; [d] calculated using the equation: $E_{HOMO} = - [E_{OX} - E_{Fc/Fc+} + 4.8]$ eV; [e] calculated from E_g and E_{HOMO} using the equation: $E_{LUMO} = (E_{HOMO} + E_g)$ (eV).

6. Computational methodology and results

The density functional theory (DFT) and time-dependent DFT (TD-DFT) calculations were performed with the Gaussian 09 program package. The density functional theory (DFT) calculations at the PBE1PBE/def2svp level was used to optimize the ground state geometries of the investigated compounds.Time-dependent density functional theory (TD-DFT) calculations was performed at the same level using the optimized ground state geometries. The electron density diagrams of molecular orbitals were generated using GaussView program. The partition orbital composition was analyzed with the Multiwfn 2.4 program. [4] The image is generated by using VMB program. [5]

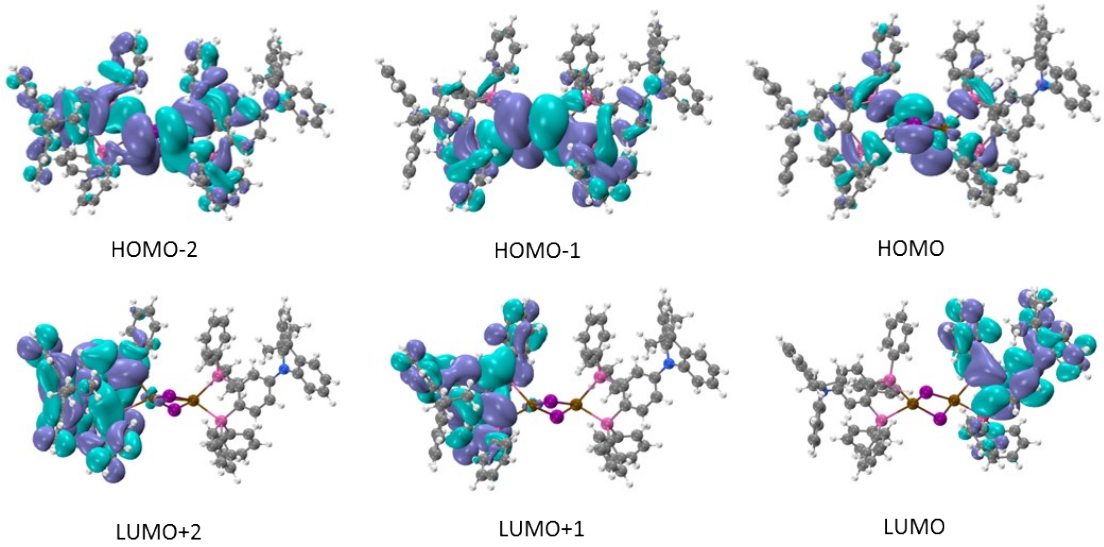

Figure S8. Contours and energy levels of the first three highest occupied (HOMO~HOMO-2) and lowest unoccupied molecular orbitals (LUMO~LUMO+2) of $Ag_2I_2(dppb\text{-}Ac)_{2.}$.

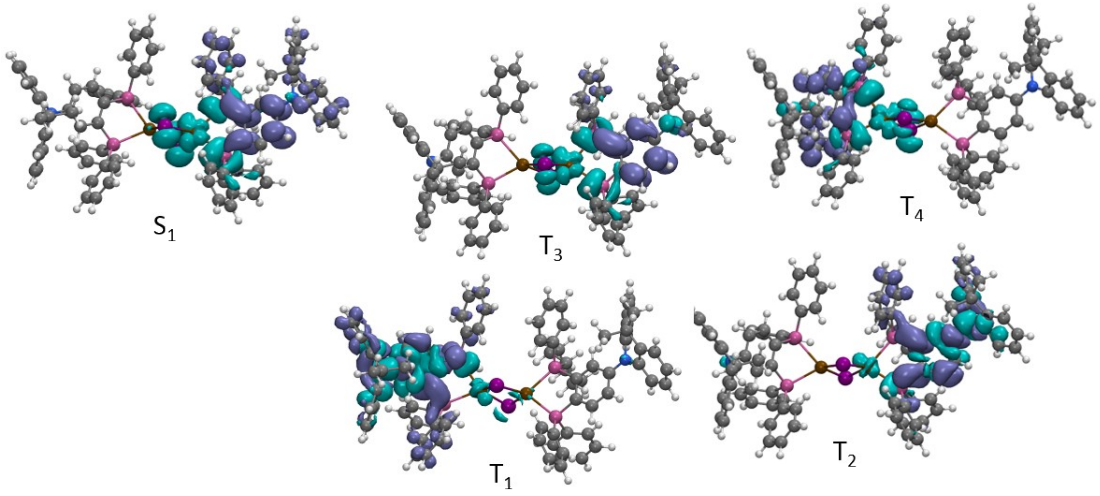

Figure S9. Contours of the S_1 and $T_1 \rightarrow T_4$ excitations for $Ag_2I_2(dppb\text{-}Ac)_{2.}$ simulated.

Table S4. Composition of the frontier orbitals of Ag_2I_2(dppb-Ac)$_2$.

	Ag	I	P	dppb	DMAC	ligand
HOMO	17.91%	31.61%	24.53%	22.91%	3.05%	50.49%
LUMO	0.35%	0.05%	8.02%	69.49	22.08%	99.59%

Table S5. Compositions of hole and electron in the S1 and T1 of Ag_2I_2(dppb-Ac)$_2$.

		Ag	I	P	dppb	DMAC	ligand
S1	hole	17.37%	23.28%	36.15%	20.42%	2.77%	59.34%
	electron	0.30%	0.01%	6.28%	72.46%	20.95%	99.69%
	difference	17.07%	23.27%	29.87%	-52.04%	-18.17	-40.35%
T1	hole	3.28%	5.58%	6.89%	37.95%	46.30	91.14%
	electron	0.68%	0.07%	7.32%	65.17%	26.77	99.26%
	difference	2.60%	5.51%	-0.43%	-27.22%	-19.54	-8.12%

Table S6. Cartesian Coordinates of Optimized Structures

S_0

Ag	-1.58341200	-1.21130500	-0.23226300
I	-0.41204200	1.05015600	1.14912600
I	0.08994400	-3.48840300	-0.43133700
Ag	1.40580200	-1.06743000	0.42976600
C	6.99285900	0.90483200	0.66737100
C	6.84782600	0.53179800	2.01731500
C	5.72344700	-0.16186900	2.44038700
C	4.68229600	-0.51458800	1.56960400
C	4.78222300	-0.07858400	0.22999900
C	5.91990800	0.61111900	-0.19366500
P	3.24445300	-1.49135100	2.16714700
P	3.39272600	-0.31980300	-0.97881900

C	3.89001000	-4.17772200	-3.55482500
C	4.89821600	-3.93715800	-2.43633500
C	4.41166100	-2.86916500	-1.45989300
C	4.07342300	-1.56142500	-2.18274200
C	3.05908200	-1.80889700	-3.30599900
C	3.55197500	-2.87842100	-4.27813800
C	2.62560500	3.58154500	-1.91247300
C	2.63609900	2.31832700	-1.32416300
C	3.40602300	1.28323500	-1.87465300
C	4.13923100	1.53360000	-3.04296000
C	4.11821400	2.79540200	-3.63592000
C	3.36700400	3.82387100	-3.06894000
C	5.61625500	-4.89722400	2.29585500
C	4.65639100	-5.90048800	2.42403300
C	3.30364300	-5.56367300	2.46603100
C	2.91135900	-4.22974100	2.37932300
C	3.87128600	-3.21331400	2.26684900
C	5.22766500	-3.55989200	2.21868300
C	3.09831500	-0.98585200	3.92421200
C	2.39112800	0.19497700	4.19477900
C	2.24085300	0.63793500	5.50643800
C	2.77688200	-0.09970900	6.56251300
C	3.46309900	-1.28465300	6.30173900
C	3.62484500	-1.72802300	4.98906200
N	8.10918300	1.60967200	0.20259600
C	8.22400800	2.02380400	-1.15012300
C	8.41486000	3.39219000	-1.40348900

C	8.41487500	4.33454200	-0.20018700
C	9.23661700	3.63529400	0.88335200
C	9.03245000	2.25498800	1.06625400
C	10.18252800	4.27569700	1.68671500
C	10.90420500	3.57506300	2.65243500
C	10.71237200	2.20462200	2.80434400
C	9.78973000	1.54155000	1.99937100
C	8.97980700	5.70896500	-0.55010600
C	6.96330800	4.52002300	0.29688200
C	8.23615700	1.09412400	-2.19360300
C	8.39555800	1.52433300	-3.50719300
C	8.57295000	2.88049300	-3.77483700
C	8.59517200	3.80018300	-2.72765600
C	-6.63554400	1.65405000	-0.41478900
C	-6.10431200	2.08478200	-1.64580300
C	-5.00750600	1.44836000	-2.21018600
C	-4.37521600	0.36213400	-1.59406200
C	-4.88017800	-0.05921800	-0.34243600
C	-5.98133400	0.58378100	0.22607200
P	-2.88441200	-0.43187900	-2.30967900
P	-4.03164100	-1.43170700	0.55360200
C	-5.33615400	-0.90818800	4.96472400
C	-5.95738500	-1.88760600	4.19215400
C	-5.59800300	-2.06067900	2.85545200
C	-4.60767400	-1.25334000	2.28258000
C	-3.96914300	-0.28405800	3.07164900
C	-4.34166400	-0.10765800	4.40149700

C	-4.75308800	-5.32725400	-0.44886400
C	-4.15937300	-4.14100600	-0.02110200
C	-4.87952900	-2.93918700	-0.05402300
C	-6.19284000	-2.94032600	-0.54226500
C	-6.78068700	-4.12742700	-0.97508700
C	-6.06329300	-5.32264500	-0.92511700
C	-5.25499000	-2.80317000	-4.74150000
C	-4.39926100	-3.86851400	-5.02097200
C	-3.11714200	-3.89183500	-4.47344600
C	-2.68814200	-2.85205500	-3.65058500
C	-3.53699000	-1.77023100	-3.37926300
C	-4.82760100	-1.75836100	-3.92383600
C	-2.24518000	0.81372300	-3.49198100
C	-1.41132000	1.81697500	-2.97510900
C	-0.86920000	2.78183700	-3.82057900
C	-1.14072800	2.74907300	-5.18879200
C	-1.95610600	1.74594700	-5.71018600
C	-2.50656200	0.78015800	-4.86754000
N	-7.72252800	2.30691500	0.17888500
C	-8.12938200	2.06379900	1.51793800
C	-8.18377700	3.16419200	2.39195700
C	-7.74763200	4.52258700	1.84330400
C	-8.35512200	4.62530100	0.44445800
C	-8.29388900	3.48283600	-0.37277900
C	-8.97253300	5.77023900	-0.06485900
C	-9.50523400	5.79096700	-1.35301600
C	-9.45366400	4.64660000	-2.14537400

C	-8.86256700	3.48812700	-1.64953600
C	-8.18876500	5.67322900	2.74439400
C	-6.20653000	4.55707600	1.73446900
C	-8.55552500	0.80076100	1.93665600
C	-8.98524500	0.60752600	3.24622500
C	-9.02427000	1.68429400	4.12787600
C	-8.64136500	2.95266300	3.69440100
H	7.60383400	0.80139500	2.75270400
H	5.64813300	-0.42907000	3.49780500
H	5.95517900	0.97817500	-1.21891200
H	2.96556000	-4.59980100	-3.12215700
H	4.27536900	-4.92646900	-4.26654700
H	5.86295700	-3.62031600	-2.87496500
H	5.09869000	-4.87198800	-1.88802700
H	5.17197900	-2.69279800	-0.68254400
H	3.50828100	-3.23629600	-0.93981400
H	5.00853700	-1.15146900	-2.61064400
H	2.83804900	-0.87385500	-3.84545800
H	2.10839200	-2.13964900	-2.85041600
H	4.44999400	-2.50899800	-4.80788000
H	2.78740000	-3.05469600	-5.05228000
H	2.02542500	4.37799800	-1.46492200
H	2.02714100	2.12737700	-0.43459600
H	4.74182000	0.74551800	-3.50034800
H	4.70008000	2.97518500	-4.54330700
H	3.35479100	4.81342300	-3.53318100
H	6.67752400	-5.15576400	2.25444900

H	4.96296600	-6.94798900	2.48199200
H	2.54393300	-6.34452800	2.54951900
H	1.84762200	-3.97555400	2.37508300
H	5.98703200	-2.78111700	2.11529800
H	1.93675900	0.75814900	3.37353400
H	1.68638300	1.55863300	5.70397400
H	2.64996800	0.24460500	7.59205200
H	3.87595500	-1.87232500	7.12574700
H	4.15957300	-2.66057200	4.79204700
H	10.36393100	5.34438600	1.56374900
H	11.63185500	4.10150000	3.27436800
H	11.29707100	1.64175900	3.53570900
H	9.67011000	0.45946600	2.07367900
H	8.95706500	6.37211900	0.32654800
H	8.36670300	6.19284300	-1.32392200
H	10.01646700	5.65081800	-0.91453800
H	6.94846300	5.17220600	1.18372100
H	6.49031200	3.56691700	0.56905400
H	6.35035000	4.98487600	-0.49055900
H	8.12942700	0.03186800	-1.96429100
H	8.40387000	0.79456700	-4.32037100
H	8.71079100	3.22488900	-4.80245200
H	8.75299300	4.85573800	-2.95364900
H	-6.52891200	2.94688400	-2.15813700
H	-4.61522400	1.83021600	-3.15633600
H	-6.31325000	0.26251300	1.21228800
H	-5.62006100	-0.77421800	6.01157300

H	-6.72820300	-2.52601100	4.63167200
H	-6.08715200	-2.83241600	2.25626800
H	-3.16503000	0.32381500	2.64384700
H	-3.83899900	0.65154700	5.00562600
H	-4.18040800	-6.25743100	-0.42175000
H	-3.12019700	-4.14285400	0.32224400
H	-6.75545500	-2.00435000	-0.59174600
H	-7.80427500	-4.11810900	-1.35840300
H	-6.52457900	-6.25210000	-1.26863900
H	-6.26466100	-2.78671200	-5.15993400
H	-4.73731400	-4.68866800	-5.65956900
H	-2.44793400	-4.73186400	-4.67492700
H	-1.69352000	-2.88983300	-3.19527400
H	-5.50424400	-0.92927300	-3.70081500
H	-1.17369400	1.83091300	-1.90596000
H	-0.21266700	3.55153400	-3.40802900
H	-0.70566200	3.50116500	-5.85190800
H	-2.16428600	1.70983500	-6.78266400
H	-3.13775100	-0.00863700	-5.28400900
H	-9.03975400	6.66910000	0.54975000
H	-9.97555400	6.70155000	-1.73132500
H	-9.89286500	4.64633000	-3.14575700
H	-8.85087100	2.57292600	-2.24451300
H	-7.85491700	6.63672800	2.33308000
H	-7.73077200	5.58255000	3.73978400
H	-9.28171300	5.70817900	2.86721500
H	-5.81466200	3.75268900	1.09752600

H	-5.75523400	4.44643100	2.73237100
H	-5.87910700	5.51779100	1.30800700
H	-8.56145000	-0.02779500	1.22653100
H	-9.30515300	-0.38535100	3.56999900
H	-9.36775700	1.54252500	5.15516900
H	-8.69872300	3.78962300	4.39177400

7. Photophysical Properties

Table S7. Φ_{PL} and emission decay time data of different concentrations of $Ag_2I_2(dppb\text{-}Ac)_{2.}$ inside PMMA films.

Emitter	Conc[a] wt%	λ_{max}[b] nm	Φ_{PL}[c] %	τ[d] µs
$Ag_2I_2(dppb\text{-}Ac)_{2.}$	5	497	51	19.4
	10	506	70	18.9
	20	517	65	13.2
	30	525	62	11.7
	50	527	59	9.1
	70	530	56	8.3
	100	532	52	7.9

[a] The concentration of doping in PMMA; [b] Photoluminescence quantum yield; [c] Photoluminescence quantum yield; [d] Emission decay time.

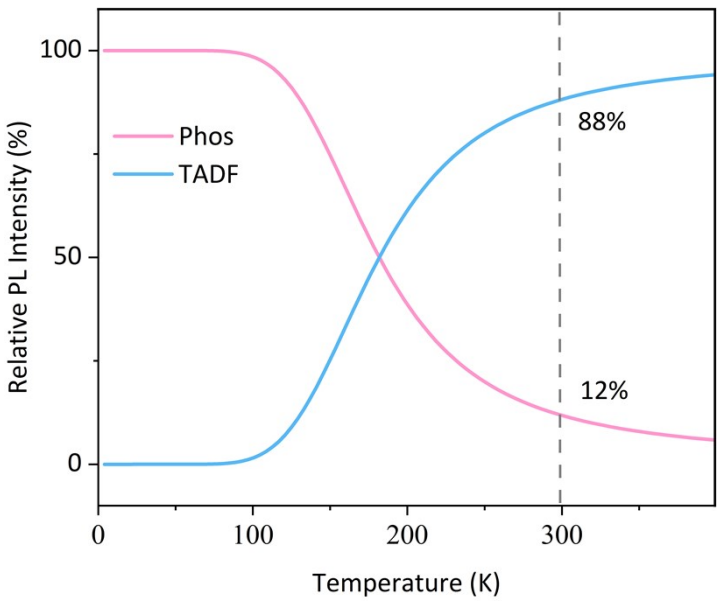

Figure S10. The contributions of TADF and phosphorescence in the total emission intensity of $Ag_2I_2(dppb\text{-}Ac)_2$ as a function of temperature, according to eqn S5 and eqn S6.

Computational methodology

Deduction and explanation for equation 1

For a system of thermally equilibrated excited states (three T_1 substates I, II, III and singlet state S_1), the temperature-dependent averaged decay time τ is given by the following expression:[6-7]

$$\tau = \frac{1 + \exp\left(-\frac{\Delta E_{II-I}}{k_B T}\right) + \exp\left(-\frac{\Delta E_{III-I}}{k_B T}\right) + \exp\left(-\frac{\Delta E_{ST}}{k_B T}\right)}{\frac{1}{\tau_I} + \frac{1}{\tau_{II}}\exp\left(-\frac{\Delta E_{II-I}}{k_B T}\right) + \frac{1}{\tau_{III}}\exp\left(-\frac{\Delta E_{III-I}}{k_B T}\right) + \frac{1}{\tau(S_1)}\exp\left(-\frac{\Delta E_{ST}}{k_B T}\right)}$$

eqn S1

The energy gap between the S_1 and T_1 states (ΔE_{ST}) is determined to be about 0.08 eV . Although it is very small, we cannot treat the S_1 and T_1 as degenerate states when compared with the splitting of the T_1 state, that is, the zero-field splitting (ZFS). For Cu(I) complexes, with the spin orbit coupling (SOC) constant of copper being about five times smaller than that of iridium or platinum, ΔE(ZFS) values of the order of 1 to 10 cm^{-1} are expected, which is significantly smaller than ΔE_{ST}.[8] Considering the energetic quasi-degeneracy of the three T_1 substates, the average decay time of T_1 is

$$\tau(T_1) = \frac{1}{3\left(\frac{1}{\tau_I} + \frac{1}{\tau_{II}} + \frac{1}{\tau_{III}}\right)}$$

eqn S2

Then, the **eqn S1** simplifies to **eqn 1**

$$\tau = \frac{1 + \frac{1}{3}\exp\left(-\frac{\Delta E_{ST}}{k_B T}\right)}{\frac{1}{\tau(T_1)} + \frac{1}{3\tau(S_1)}\exp\left(-\frac{\Delta E_{ST}}{k_B T}\right)}$$

Relative contributions of TADF and phosphorescence

In order to evaluate the relative contributions of TADF and phosphorescence, we estimate the percentage of the intensity originating from the singlet $I(S_1)$ and from the triplet state $I(T_1)$ relative to the total intensity I_{tot} in dependence of the temperature.[9] The intensity is proportional to the population of the individual state N and to the corresponding radiative rate constant k_r, so we can obtain

$$I(S_1) = \alpha N(S_1) k_r(S_1) = \alpha N(S_1) \Phi_{PL}(S_1) \tau(S_1)^{-1}$$

eqn S3

$$I(T_1) = \alpha N(T_1) k_r(T_1) = \alpha N(T_1) \Phi_{PL}(T_1) \tau(T_1)^{-1}$$

eqn S4

Herein, α is the proportionality constant that is same in both the equations. For rough estimates, we assume that the quantum yields $\Phi_{PL}(S_1)$ and $\Phi_{PL}(T_1)$ do not depend on the temperature, and we use the Φ_{PL} values determined at 300 K and 77 K, respectively (Table 2). Assuming that the populations of both states follow a Boltzmann distribution (fast equilibration), the relative intensities can be expressed as follows

$$\frac{I(T_1)}{I_{tot}} = \frac{I(T_1)}{I(S_1) + I(T_1)} = [1 + \frac{I(S_1)}{I(T_1)}]^{-1} = [1 + \frac{\alpha N(S_1) \Phi_{PL}(S_1) \tau(S_1)^{-1}}{\alpha N(T_1) \Phi_{PL}(T_1) \tau(T_1)^{-1}}]^{-1}$$
$$= [1 + \frac{N(S_1) \Phi_{PL}(S_1) \tau(T_1)}{N(T_1) \Phi_{PL}(T_1) \tau(S_1)}]^{-1} = [1 + \frac{\Phi_{PL}(S_1) \tau(T_1) g(S_1)}{\Phi_{PL}(T_1) \tau(S_1) g(T1)} \exp(-\frac{\Delta E_{ST}}{k_B T})]^{-1}$$

eqn S5

$$\frac{I(S_1)}{I_{tot}} = 1 - \frac{I(T_1)}{I_{tot}} = 1 - [1 + \frac{\Phi_{PL}(S_1) \tau(T_1) g(S_1)}{\Phi_{PL}(T_1) \tau(S_1) g(T1)} \exp(-\frac{\Delta E_{ST}}{k_B T})]^{-1}$$

eqn S6

where $g(S_1) = 1$ and $g(T_1) = 3$ are the degeneracy factors for the singlet and the triplet states, respectively. The splitting of the T_1 state, that is, the zero-field splitting (ZFS), is distinct in organo-transition-metal compounds due to the high metal participation and large spin-orbit coupling. So, we take into account the degeneracy factors for the singlet and the triplet states $g(S_1) = 1$ and $g(T_1) = 3$ in evaluating the populations of the two states (Boltzmann distribution). The plots shown in S9 can be obtained using eqn S5 and eqn S6, in which the parameters have been determined by eqn 1 (see Figure. 4e). As a result, the relative contributions of TADF and phosphorescence are depicted visually in Figure. S9.

9.NMR Spectra

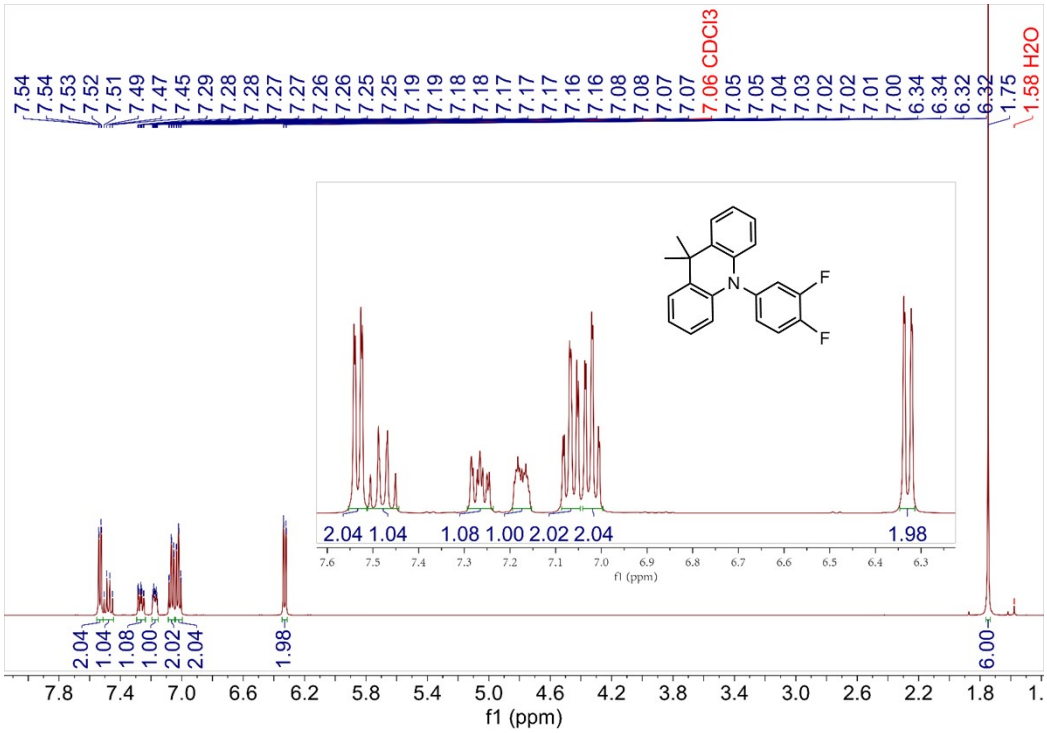

Figure S11. ^{1}H NMR spectrum of DMAC-PhF_2 in $CDCl_3$.

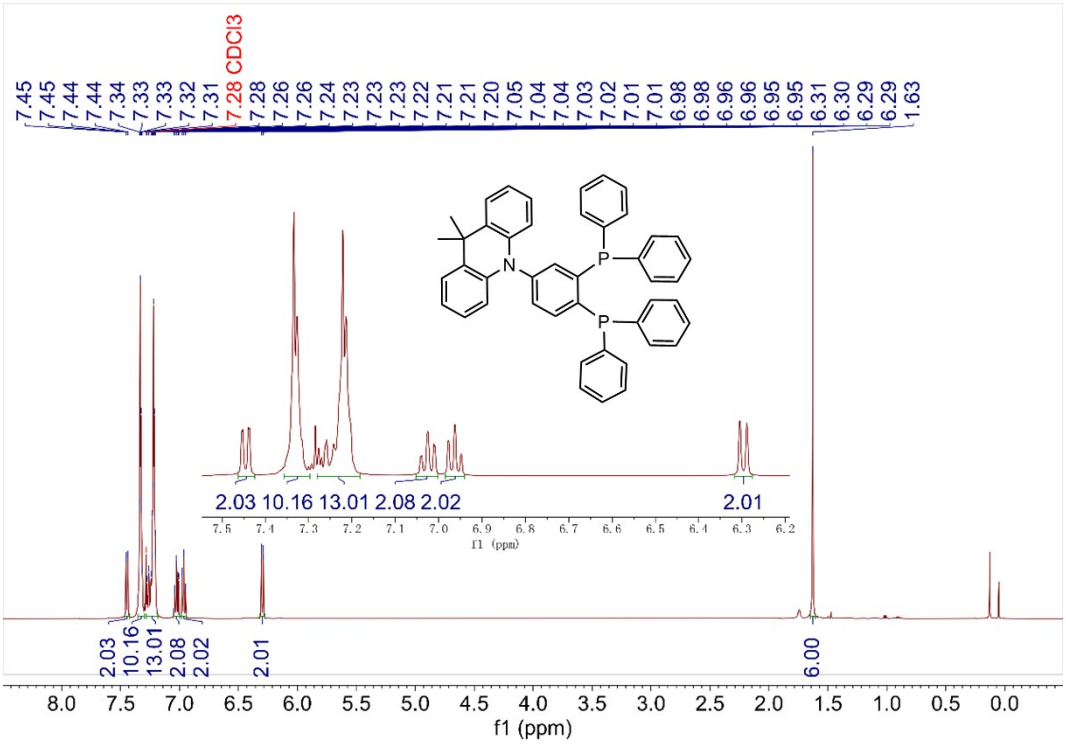

Figure S12. ^{1}H NMR spectrum of dppb-Ac in $CDCl_3$.

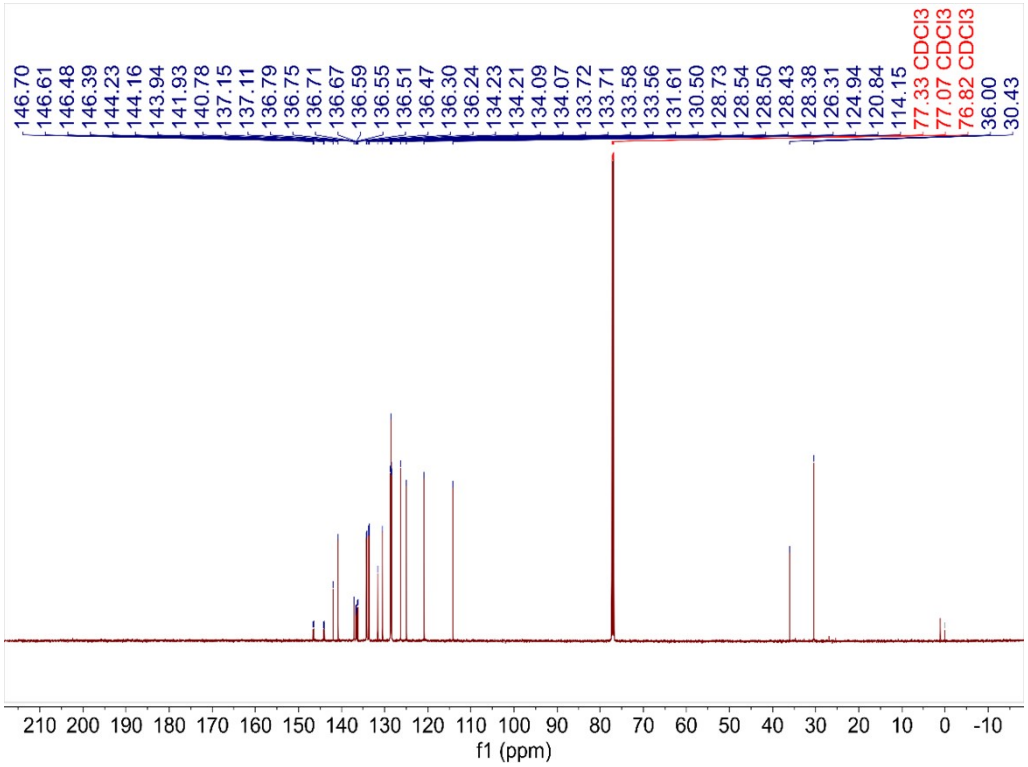

Figure S13. ^{13}C NMR spectrum of dppb-Ac in $CDCl_3$.

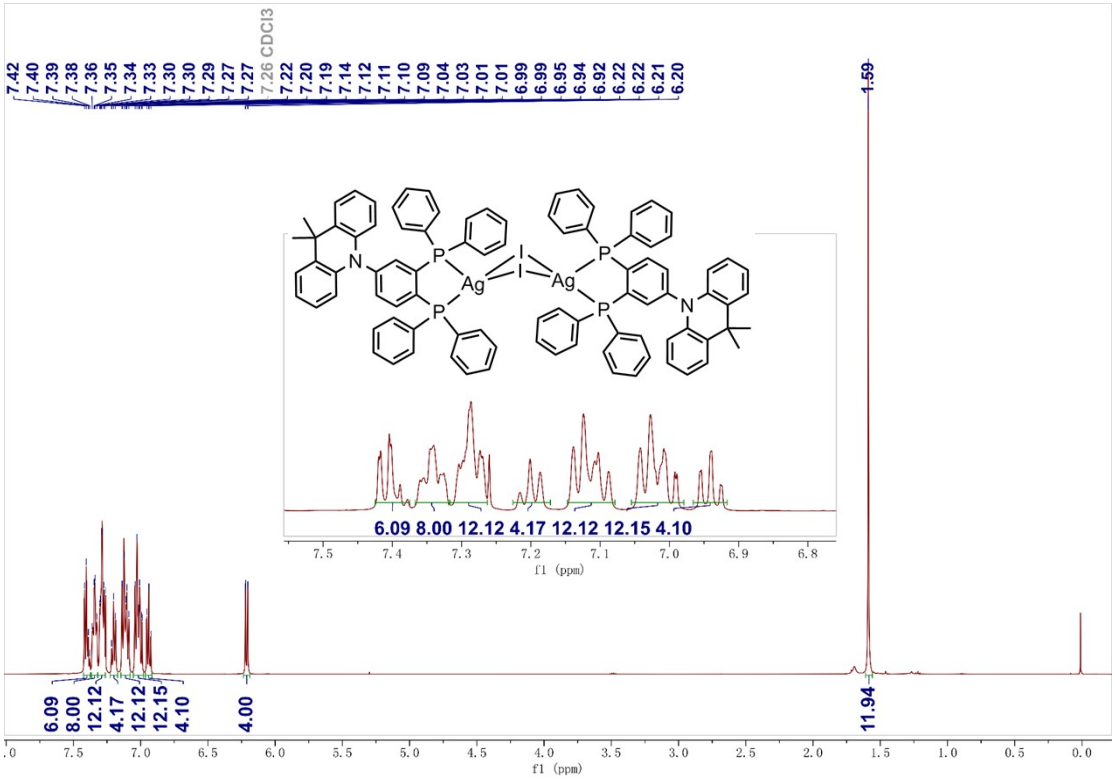

Figure S14. ^{1}H NMR spectrum of Ag_2I_2(dppb-Ac)$_2$ in $CDCl_3$.

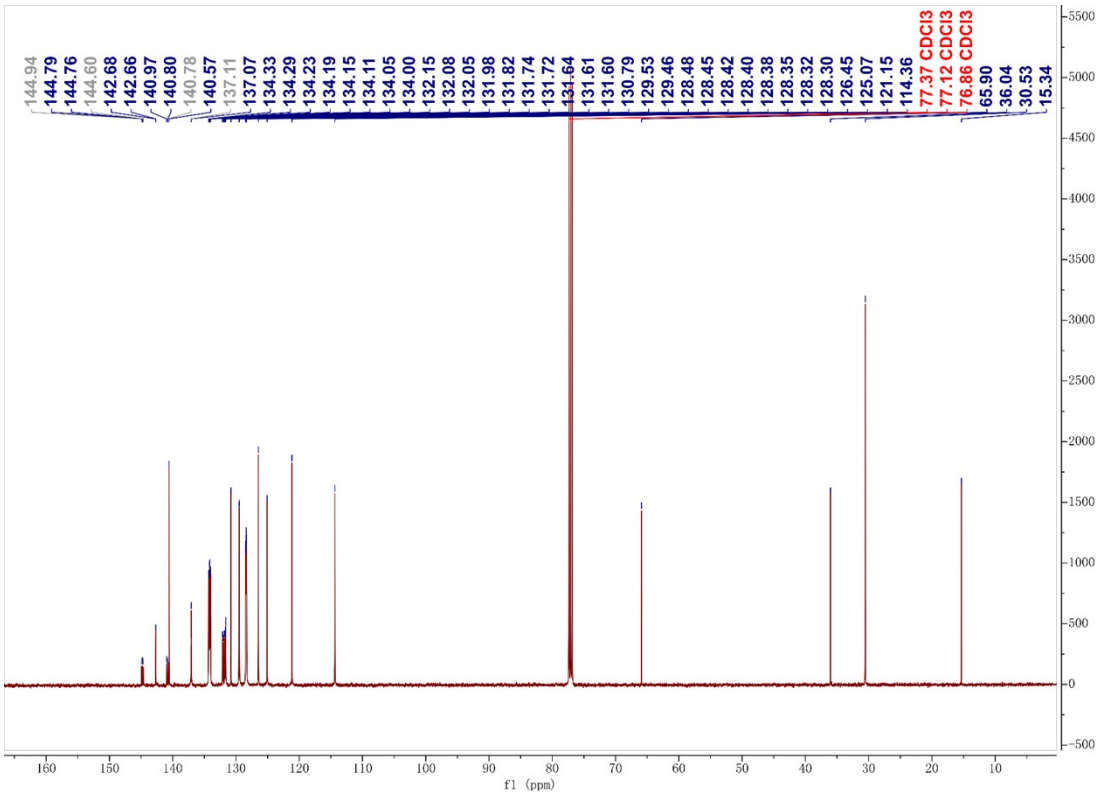

Figure S15. ^{13}C NMR spectrum of Ag_2I_2(dppb-Ac)$_2$ in $CDCl_3$.

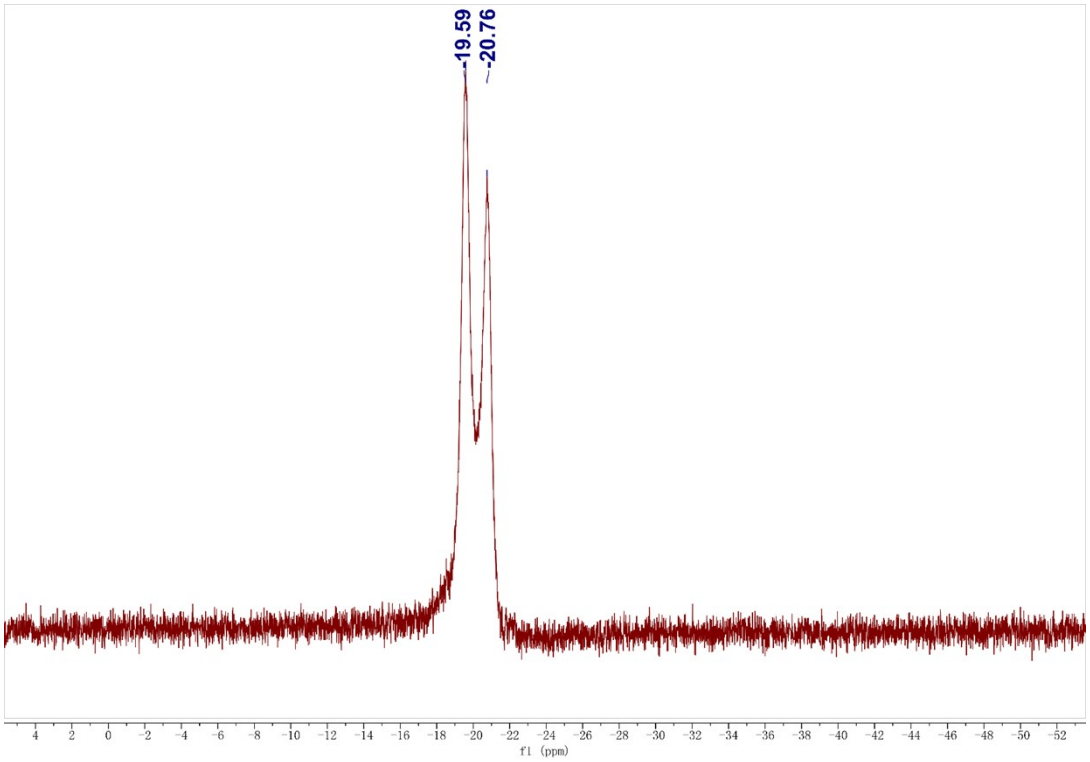

Figure S16. ^{31}P NMR spectrum of $Ag_2I_2(dppb\text{-}Ac)_2$ in $CDCl_3$.

1. Jia, J. H.; Liang, D.; Yu, R.; Chen, X. L.; Meng, L.; Chang, J. F.; Liao, J. Z.; Yang, M.; Li, X. N and Lu, C. Z., Coordination-Induced Thermally Activated Delayed Fluorescence: From Non-TADF Donor–Acceptor-Type Ligand to TADF-Active Ag-Based Complexes. *Chem Mater* **2019**, *32* (1), 620-629.
2. Kang, L.; Chen, J.; Teng, T.; Chen, X.-L.; Yu, R and Lu, C.-Z., Experimental and theoretical studies of highly emissive dinuclear Cu(I) halide complexes with delayed fluorescence. *Dalton Trans* **2015**, *44* (25), 11649-11659.
3. Espinoza, E. M.; Clark, J. A.; Soliman, J.; Derr, J. B.; Morales, M.; Vullev, V. I., Practical Aspects of Cyclic Voltammetry: How to Estimate Reduction Potentials When Irreversibility Prevails. *J Electrochem Soc* **2019**, *166* (5), H3175-H3187.
4. Lu, T and Chen, F., Multiwfn: a multifunctional wavefunction analyzer. *J Comput Chem* **2012**, *33* (5), 580-92.
5. Humphrey, W.; Dalke, A and Schulten, K., VMD: Visual Molecular Dynamics. *J Mol Graph*, **1996**, *14*, 33-38.
6. Leitl, M. J.; Krylova, V. A.; Djurovich, P. I.; Thompson, M. E.; Yersin, H., Phosphorescence versus thermally Activated Delayed Fluorescence. Controlling Singlet-triplet Splitting in Brightly Emitting and Sublimable Cu(I) compounds. *J Am Chem Soc* **2014**, *136* (45), 16032-16038.
7. Chen, X. L.; Yu, R.; Zhang, Q. K.; Zhou, L. J.; Wu, X. Y.; Zhang, Q.; Lu, C. Z., Rational Design of Strongly Blue-Emitting Cuprous Complexes with Thermally Activated Delayed

Fluorescence and Application in Solution-Processed OLEDs. *Chem Mater* **2013**, *25* (19), 3910-3920.

8. Yersin, H.; Rausch, A. F.; Czerwieniec, R.; Hofbeck, T.; Fischer, T., The triplet state of organo-transition metal compounds. Triplet harvesting and singlet harvesting for efficient OLEDs. *Coord Chem Rev* **2011**, *255* (21-22), 2622-2652.
9. Leitl, M. J.; Kuchle, F. R.; Mayer, H. A.; Wesemann, L.; Yersin, H., Brightly Blue and Green Emitting Cu(I) Dimers for Singlet Harvesting in OLEDs. *J Phys Chem A* **2013,** *117* (46), 11823-11836.